Acta Chemica Scandinavica, 1999: 53: 7–14
Printed in UK – all rights reserved

ACTA
CHEMICA SCANDINAVICA
ISSN 0904–213X

NMR Spectroscopic and Potentiometric Study on Complexation Thermodynamics of Some *N,N'*-Bis(2-hydroxyethyl)piperazine Complexes

Vesa Hietapelto,* Risto S. Laitinen, Jouni Pursiainen and Erkki Rahkamaa

Department of Chemistry, University of Oulu, Linnanmaa, FIN-90570 Oulu, Finland

Hietapelto, V., Laitinen, R. S., Pursiainen, J. and Rahkamaa, E., 1999. NMR Spectroscopic and Potentiometric Study on Complexation Thermodynamics of Some *N,N'*-Bis(2-hydroxyethyl)piperazine Complexes. – Acta Chem. Scand. 53: 7–14. © Acta Chemica Scandinavica 1999.

The complex formation equilibria between *N,N'*-bis(2-hydroxyethyl)piperazine and alkaline-earth(II), praseodymium(III), nickel(II), copper(II) and zinc(II) ions were studied with potentiometric techniques over the pH range 2.4–9.6 in 0.10 mol dm^{-3} NaCl at 25 °C. The data indicate the formation of the species $[ML]^{2+/3+}$, $[M(HL)]^{3+/4+}$ and the hydrolysis of copper(II) (aq). The protonation of the ligand was also studied by ^1H NMR spectroscopy in 0.10 mol dm^{-3} NaCl (aq) at 24 °C. These data, together with $^{13}C\{^1H\}$ NMR spectroscopic data, indicate equatorial–equatorial and equatorial–axial conformations of 2-hydroxyethyl side chains with respect to the six-membered piperazine ring. The ring inversion of the piperazine ring was studied by ^1H NMR spectroscopy in 1:1 (v:v) acetone–methanol solution over the temperature range 40 to −90 °C.

Copper, zinc, nickel, magnesium and calcium ions are very important to human beings. Magnesium is more abundant within cells, while calcium (together with sodium and chloride) is dominant in the extracellular space. Copper, zinc and nickel are also important in many metalloenzymes.[1] Strontium, barium and praseodymium ions are useful models of large hard metal ions.

Piperazine and its *N*-substitution derivatives have pharmacological applications as anthelmintics, sedatives and local anaesthetics.[2] Au^{III}, Os^{IV}, Pd^{II}, Pt^{IV} and Pt^{II} *N,N'*-bis(2-hydroxyethyl)piperazine complexes have antitumoral activity against lymphoid leukemia L1210.[3] It is therefore important to understand the complex formation of piperazine with a variety of metal ions. The published information on thermodynamic data for the protonation or the complex formation of *N,N'*-bis(2-hydroxyethyl)piperazine is sparse. Furthermore, Vega and Bates[4] mentioned that in the case of *N*-(2-hydroxyethyl)-piperazine-*N'*-ethanesulfonic acid the acid–base behaviour of nitrogen bound to the 2-hydroxyethyl group is not easily predicted. Furthermore, the piperazine unit itself can be used as a spacer. The resulting macrocycle may be water-soluble because of the piperazine nitrogen atoms, as exemplified by nitrogen containing crown ethers as well as aromatic and amino-based macrocycles.[5–14] Instead of the rigid aromatic system the piperazine offers an aliphatic spacer that is reorganized and hence conformationally flexible.

* To whom correspondence should be addressed.

N,N'-Bis(2-hydroxyethyl)piperazine is water soluble and therefore suitable for traditional potentiometric titration in a constant ionic medium. The potentiometric titration has proved to be one of the most suitable techniques in studying complicated complex formation equilibria in solution. NMR spectroscopy was used to study conformational and dynamic equilibria in solutions.

Experimental

Reagents and solutions. Stock solutions of alkaline-earth metal(II), copper(II), zinc(II) and nickel(II) ions were prepared from their respective chlorides (Merck) and praseodymium(III) from Pr_6O_{11} (Typpi OY) dissolved in hydrochloric acid. These stock solutions were standardized by titration with EDTA as well as by cation exchange chromatography.[15] *N,N'*-Bis(2-hydroxyethyl)-piperazine (Aldrich) was used without further purification. The purity of the compound was determined by ^1H NMR spectroscopy and by titration with standardized NaOH solution. Hydrochloric acid (Baker) was standardized by titration with tris(hydroxymethyl)aminomethane (TRIS) using a mixture of bromocresol green and methyl red (3:2) as an indicator. The NaOH stock solution was prepared by dissolving NaOH granules (Merck) in boiling distilled water. It was stored in a high-density polyethene bottle fitted with a carbon dioxide (soda lime) trap. The NaOH stock solution was

standardized by titration against potassium hydrogen phthalate using phenolphthalein as an indicator.

Potentiometric studies. The potentiometric studies were carried out in an inert atmosphere [commercial argon passed through 10% (w/w) H_2SO_4, 10% (w/w) NaOH and background electrolyte] at 25 ± 0.1 °C using a locally constructed automatic titration system (TIT5 program)[16] involving a Methrohm 665 piston burette as well as Orion 91-01sc glass electrode and Orion 9002 Ag/AgCl (s) double junction reference electrode. The ligand and metal ion concentrations as well as the pH range are given in Table 1. Every titration was started with the calibration of the electrode system by titration of 30 or 40 cm^3 of E_0-solution (0.090 mol dm^{-3} and 0.010 mol dm^{-3} with respect to NaCl and HCl) with CO_2-free 0.10 mol dm^{-3} NaOH solution. These data were employed to obtain the values of E_0 and E_j in the Nernst equation

$$E = E_0 + 59.16 \log h + E_j \quad (1)$$

The liquid junction potential E_j assumed a significant value at pH < 2.5. The titrations, however, were mainly carried out in conditions where the liquid junction potential was negligible. When needed, the following values for the liquid junction potential ($E_j = jh$) were used [j(acid) = −512 mV M^{-1}, j(alk) = 239 mV M^{-1} and $pk_w = 13.775$] consistent with the literature values.[17] The acidified solution of the ligand (H_2L^{2+}) was titrated with NaOH and that of the partially protonated ligand with NaOH and HCl to obtain the protonation constants and the exact ligand concentration. Solutions containing the acidified ligand and the metal ion were titrated with NaOH to high pH to determine the stability constants of the metal complexes. Because of the aging the ligand solution had to be replaced every 2–3 weeks.

NMR studies. The ^{1}H NMR spectroscopic measurements were carried out on a Bruker AM 200 spectrometer operating at 200.13 MHz. The sample temperature was 24 ± 1 °C in each case. In order to reach a sufficiently good signal-to-noise ratio, 128 FIDs were accumulated by applying a spectral with of 3.5 kHz, resulting in a digital resolution of 0.365 Hz/point. The protonation constants were determined by NMR measurements using batch techniques. The pH of each sample solution (standardized stock solution) was adjusted with concentrated HCl and NaOH solutions and monitored with a combination electrode (Schott N6280) and pH-meter (CG 836) (pH 4.01 and 6.87 buffers) at room temperature (about 24 °C). The spectra were measured in a 5-mm tube directly from the water solution within a day after the pH adjustment to mimic the potentiometric titration. C_6D_6 was used as an external ^{2}H lock and TMS as an external reference. Solvent peak suppression was carried out by the presaturation method.

In order to facilitate the assigment of the ^{1}H spectra, another series of measurements was carried out in D_2O. The pD of each sample solution (1 g ligand in 10 cm^3 D_2O) was adjusted with DCl and NaOD (Sigma) solutions and monitored with a combination electrode (Schott N6280) and pH-meter (CG 836) (pH 4.01 and 6.87 buffers) at room temperature.

The variable-temperature ^{1}H NMR spectroscopic measurements in the range 40 to −90 °C were carried out on a Bruker DPX 400 spectrometer operating at 400.13 MHz. Spectra were measured directly from a 1 : 1 (v : v) acetone–methanol solution in a 5-mm tube. Acetone-d_6 served as the external ^{2}H lock and TMS as the external reference. The acetone–methanol mixture was used to increase the solubility of the neutral ligand (non-protonated) and to enable the recording of spectra at lower temperatures. Acetone and methanol resonances partially obscured the signals of interest. The temperature of the samples were allowed to settle for 30 min after every temperature change. The spectra were processed without any window function.

The $^{13}C\{^1H\}$ NMR spectroscopic measurements were carried out on a Bruker DPX 400 spectrometer operating at 100.62 MHz. In order for a sufficiently good signal-to-noise ratio to be attained, 2400 FIDs were accumulated by applying a spectral with of 30 kHz, pulse width 5.0 μs, a pulse delay of 5.8 s and a digital resolution of 0.611 Hz/point. The pH of each sample solution (4 g ligand in 20 cm^3 H_2O) was adjusted with HCl and NaOH solutions and monitored with a combination electrode (Schott N6280) and pH-meter (CG 836) (pH 4.01 and 6.87 buffers) at room temperature. The spectra were measured in a 10-mm tube within a day after the pH

Table 1. Experimental parameters: n_T = number of titrations, n_P = number of titration points, C_L = ligand concentration, C_M = metal ion concentration, M/L = metal to ligand concentration ratio.

Compound	n_T/n_P	M/L	C_L/mmol dm^{-3}	C_M/mmol dm^{-3}	pH range
L, protonation, pot	3/138	—	3.203–3.367	—	2.4–9.6
L, protonation, ^{1}H NMR	1/13	—	10.755	—	2.4–9.0
Mg^{II}	3/55	1:1, 2:1, 5:1	0.821–1.639	1.471–4.091	3.0–8.6
Ca^{II}	6/131	1:2, 1:1, 2:1, 5:1	0.817–1.797	0.910–3.599	2.5–8.7
Sr^{II}	3/50	1:1, 2:1, 5:1	0.816–1.634	1.688–4.273	3.2–8.7
Ba^{II}	3/48	1:1, 2:1, 5:1	0.817–1.634	1.463–4.052	3.2–8.7
Pr^{III}	6/109	1:1, 2:1, 5:1	0.812–3.308	1.472–6.445	2.5–7.5
Ni^{II}	3/48	1:1, 2:1, 5:1	0.817–1.634	1.516–4.199	3.2–8.0
Cu^{II}	4/73	1:2, 1:1, 2:1, 5:1	0.817–1.827	0.859–4.010	2.5–5.1
Zn^{II}	3/41	1:1, 2:1, 5:1	0.817–1.634	1.427–3.952	3.2–7.4

adjustment. C_6D_6 was used as an external ^2H lock and TMS as an external reference.

Calculations

Potentiometric titrations and ^1H NMR measurements were carried out with the ligand concentration range indicated in Table 1. The protonation constants of the ligand and the stability constants of complexes were calculated from the potentiometric data with the program LETAGROPVRID, version ETITR.[18–20] The best fit to the experimental data was determined by minimizing the error square sum $U=\Sigma(H_{calc}-H_{exp})^2$, where H is the total hydrogen ion concentration. Every metal ion–ligand system has been modelled by the computer program SOLGASWATER.[21] The program calculates the equilibrium concentrations of all assumed species if total or free concentrations of the components and stability constants for the present model are given. Theoretical $Z(A/B)$ (the average number of protons bound to each ligand) versus $-\log[H^+]$ curves were calculated using this program to evaluate the correctness of the model.[22]

The overall protonation constants from ^1H NMR data (pH, δ_H) were calculated with the program SIGMAPLOT.[23] It is a nonlinear curve-fitting program, which calculates the best sets of parameters by minimizing the square sum $U=\Sigma(\delta_{calc}-\delta_{exp})^2$. Protonation equilibria can be described by a general reaction:

$$rH^+ + L^{n-} \rightleftharpoons H_rL^{r-n} \qquad \beta_{1r} \tag{2}$$

Because the exchange between the free ligand and bonded protons is rapid with respect to the NMR timescale, only a time-averaged chemical shift can be observed.

The observed chemical shift is given by:

$$\delta_{exp} = \Sigma\, \delta_{H,L} X_{H,L} \tag{3}$$

where

$$X_{H,L} = [H_rL]/C_L \tag{4}$$

From the law of mass action the following relations can be obtained:

$$C_L = [L^{n-}] + \Sigma\, \beta_{1r}[H^+]^r[L^{n-}] \tag{5}$$

$$[H_rL] = \beta_{1r}[H^+]^r[L^{n-}] \tag{6}$$

Combining eqns. (3)–(6) gives

$$\delta_{exp} = (\delta_L + \Sigma\, \beta_{1r}[H^+]^r\delta_{H,L})/(1 + \Sigma\, \beta_{1r}[H^+]^r) \tag{7}$$

In the region of slow exchange, in which the spectrum is no longer sensitive to the kinetic effect, the values of $\delta\nu$ are determined. Without a complete line shape analysis the rate constant k_{coal} at the coalescence temperature, T_C/K, can be calculated from the equation[24]

$$k_{coal} = \pi\delta\nu/\sqrt{2} = 2.22\,\delta\nu \tag{8}$$

where $\delta\nu$ denotes the chemical shift difference (in Hz) between two equally populated sites. This enables the use of the Eyring equation to make a quick evaluation of the energy barrier for the ring inversion process at the coalescensce temperature, T_C/K:

$$\Delta G^{**} = RT_C[22.96 + \ln(T_C/\delta\nu)] \tag{9}$$

Enthalpy and entropy changes of the process can be evaluated from eqn. (10):

$$\ln(k/T) = 23.76 - (\Delta H^{**}/RT) + (\Delta S^{**}/R) \tag{10}$$

Results and discussion

Protonation. The logarithms of the protonation constants are presented in Table 2. The overall protonation constant of *N,N'*-dimethylpiperazine[25] is slightly larger than that of *N,N'*-bis(2-hydroxyethyl)piperazine, because the negative inductive effect of the 2-hydroxyethyl group lowers the basicity of nitrogen compared to the methyl derivative.

The ^1H NMR chemical shift data of the 2-hydroxyethyl methylene protons (**a**) and (**a'**) (Fig. 1) indicate slightly different constants when compared to the values obtained from potentiometric data. The conditions involved in the ^1H NMR measurements are slightly different (concentration, temperature, time and pH) from those during the the potentiometric titrations, and they seem to have an effect on the values. The difference can further be explained as follows: The calculation is very sensitive to the changes in the chemical shift of the proton. The protonation constants calculated from resonance (**a**) differ from the constants calculated from (**a'**). Log β_{11} calculated from resonance (**a**) is slightly greater than the one calculated from (**a'**). Log β_{12} exhibits the opposite trend. The potentiometric titration cannot distinguish small differences between the two protonation constants. Only a single constant is obtained.

Complex formation. Logarithms of the overall stability constants are shown in Table 3. The complexation of

Table 2. The protonation constants β_{qr} ($\pm\sigma$)[a] and K_{qr}[a] of *N,N'*-bis(2-hydroxyethyl)piperazine at 25 °C and I = 0.10 mol dm^{-3} NaCl, as determined using potentiometric techniques and ^1H NMR spectroscopy.

	log β_{11}	log β_{12}	log K_{11}	log K_{12}	U
Potentiometric	7.78 (0.004)	11.52 (0.004)	7.78	3.74	1.9×10^{-3}
^1H NMR, (**a**)[b]	7.72 (0.02)	11.61 (0.02)	7.72	3.89	3.8
^1H NMR, (**a'**)[b]	7.65 (0.04)	11.67 (0.05)	7.65	4.02	9.4
Potentiometric[c]	8.13	12.31	8.13	4.18	—

[a] β_{qr} refers to the reaction $qL+rH=L_qH_r$ and K_{qr} refers to the reaction $L+H=LH$ and $LH+H=LH_2$. [b] ^1H NMR spectroscopic measurements have been carried out at 24 °C. [c] See Ref. 25 for the potentiometric determination of the protonation constants of *N,N'*-dimethylpiperazine at 25 °C and I = 0.10 mol dm^{-3} KNO_3.

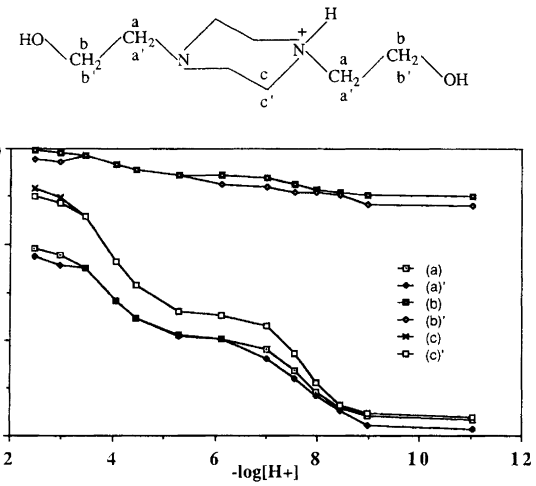

Fig. 1. Plot of the ^1H chemical shift (in Hz) versus $-\log[H^+]$ of *N,N'*-bis(2-hydroxyethyl)piperazine at 24 °C and $I = 0.10$ mol dm^{-3} NaCl.

Table 3. The overall stability constants, β_{pqr} ($\pm\sigma$),[a] of alkaline-earth(II), praseodymium(III), nickel(II), copper(II), zinc(II) and *N,N'*-bis(2-hydroxyethyl)piperazine complexes at 25 °C and $I = 0.10$ mol dm^{-3} NaCl.

Metal ion	$\log \beta_{110}$	$\log \beta_{111}$	*U*
Mg^{II}	2.12 (0.017)	—	1.1×10^{-4}
Ca^{II}	2.03 (0.007)	—	1.8×10^{-5}
Sr^{II}	1.97 (0.014)	—	8.0×10^{-5}
Ba^{II}	2.04 (0.037)	9.76 (0.060)	4.8×10^{-4}
Pr^{III}	2.33 (0.034)	9.18 (0.057)	2.6×10^{-4}
Ni^{II}	2.60 (0.037)	9.78 (0.057)	3.5×10^{-3}
Cu^{II}	—	10.18 (0.060)	4.5×10^{-2}
Zn^{II}	2.67 (0.030)	9.93 (0.034)	9.2×10^{-4}

[a] β_{pqr} refers to the reaction $pM + qL + rH = M_pL_qH_r$.

N,N'-bis(2-hydroxyethyl)piperazine with alkaline-earth(II), praseodymium(III), nickel(II), copper(II) and zinc(II) ions is quite weak. This is exemplified by the Zn^{II}–ligand (1:1) system, where at most 25% of the ligand has complexed (Figs. 2 and 3). The mono-protonated complex is apparently present in every system,

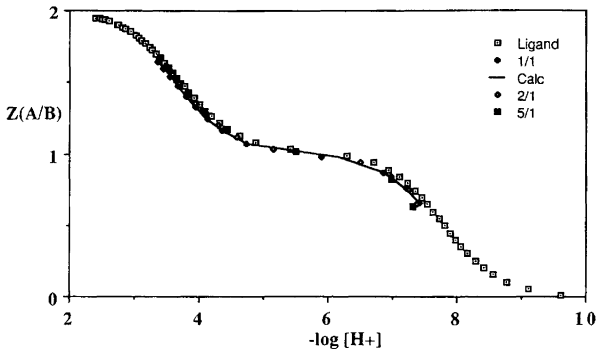

Fig. 2. *Z*(A/B) (the average number of protons bound to each ligand) plotted versus $-\log[H^+]$ for Zn^{II}–*N,N'*-bis(2-hydroxyethyl)piperazine and calculated data for a 1:1 metal–ligand concentration ratio.

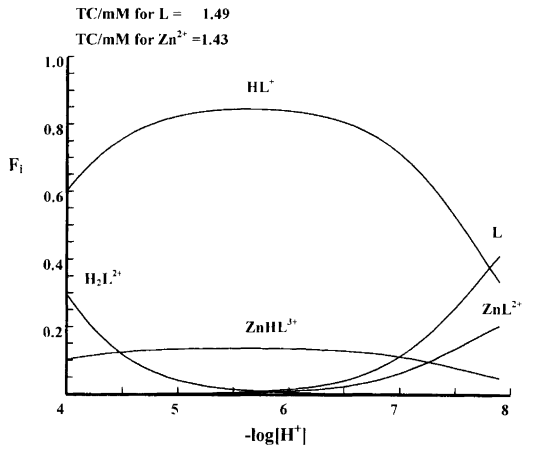

Fig. 3. The distribution diagram for individual Zn^{II}–*N,N'*-bis(2-hydroxyethyl)piperazine titration at a 1:1 metal–ligand concentration ratio.

but it is not possible to calculate the stability constants for Mg^{II}–Sr^{II} because of the weakness of the complexation. The existence of $[Cu^{II}(HL)]^{3+}$ is quite uncertain, as seen from the higher *U*-value when compared to other systems, even though the stability constant of $[Cu^{II}(HL)]^{3+}$ is expected to be the largest for the protonated complexes. This is explained by the predominance of the hydrolysis of Cu^{II}(aq). The protonated complexes of barium(II) and nickel(II) are of comparable strength.

The stability of the alkaline-earth metal complexes does not follow the well known trends that are characteristic for polyaminocarboxylic acids, polycarboxylic acids, hydroxycarboxylic acids or some other anions.[26] The stability of the complexes seems to decrease when going down the group; however, Ba^{II} does not follow this trend. Its stability constant is similar to the that of the Ca^{II} complex. The differences in the stability constants, however, are quite small, and the average value of $\log \beta$ is about 2 for all alkaline-earth metal ions. The stability of the $[Pr^{III}L]^{3+}$ complex is higher than those of the alkaline-earth metal complexes, but lower than that of the transition metal complexes. This is because the transition metal ions have stronger covalent effects than lanthanoids and alkaline-earth metal ions. The higher charge of lanthanoids compared to alkaline-earth metal ions partly explains the stability constant differences among hard metal ions. Zn^{II} forms a slightly stronger [ML] complex than Ni^{II}, but Cu^{II} does not form a [ML] complex. The stepwise stability constants ($\log K$) of the protonated complexes are not very much smaller than those of the [ML] complexes, except for the Pr^{III} complex. This mainly indicates monodentate coordination through one nitrogen donor atom, not chelate formation through two nitrogen atoms.

The hydroxyl group does not seem to deprotonate. Therefore the ligand is more likely to be monodentate, but the coordination through hydroxyl group is very weak. With the exception of $[Ba^{II}(HL)L]^{3+}$ the experi-

mental data do not indicate the presence of the $[ML_2]$ or [M(HL)L] complexes in any of the systems studied in this paper. The log β value of $[Ba^{II}(HL)L]^{3+}$ is 12.45 ± 0.06. The inclusion of $[Ba^{II}(HL)L]^{3+}$, however, did not improve the model according to the $Z(A/B)$ analysis. Similarly, the inclusion of different polymeric species in the model did not improve the fit between experimental and calculated data. It is therefore unlikely that polymeric species are present even in an excess of the metal ions. *N,N'*-Dimethylpiperazine forms [ML] and $[ML_2]$ complexes but no [M(HL)] complex with Ag^I, and stability constants are 2.20 and 3.46.[27] The stability constant of the $[Ag^IL]$ complex is lower than that of *N,N'*-bis(2-hydroxyethyl)piperazine transition metal complexes, which is natural because of lower charge of the Ag^I ion. The existence of the $[ML_2]$ complex perhaps arises because of steric reasons: the shorter methyl chains do not form such a crowded structure as do 2-hydroxyethyl chains.

NMR spectroscopy. The identification of the ^1H resonances is based on Ref. 28. The ^1H NMR spectra in D_2O are shown in Fig. 4 and the corresponding data in Table 4. The resonances due to the 2-hydroxyethyl side chains appear as triplets of A_2X_2 at high pD and are transformed into second-order AA'XX' multiplets as pD is decreased. Simultaneously, the wide signal that was assigned to the methylene protons of the piperazine ring transformed into a sharp singlet.

The ^1H NMR spectra are shown in Fig. 5 as a function of pH. During the first protonation (pH 9–6) both side-chain methylene signals are split into triplets (**a**) and (**b**)

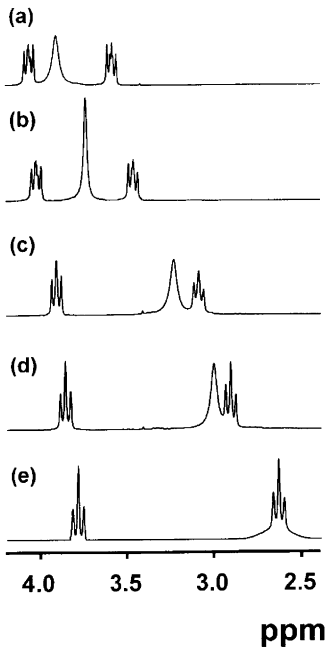

Fig. 4. ^1H NMR spectra at 200 MHz of *N,N'*-bis(2-hydroxyethyl)piperazine plotted versus pD in D_2O: (a) 1.89, (b) 3.70, (c) 5.70, (d) 7.83 and (e) 10.98.

Table 4. ^1H NMR of *N,N'*-bis(2-hydroxyethyl)piperazine in D_2O.

pD	Multiplicity	δ_H (ppm)	^3J (H,H)/Hz
10.98	Triplet	3.79	6.0
	Singlet (wide)	2.63	
	Triplet	2.63	6.0
7.83	Triplet	3.86	5.8
	Singlet	3.00	
	Triplet	2.90	5.8
5.70	Multiplet	3.91	Higher-order system
	Singlet	3.23	
	Triplet	3.09	Higher-order system
3.70	Multiplet	4.01	Higher-order system
	Singlet	3.73	
	Multiplet	3.45	Higher-order system
1.89	Multiplet	4.06	Higher-order system
	Singlet	3.91	
	Multiplet	3.59	Higher-order system

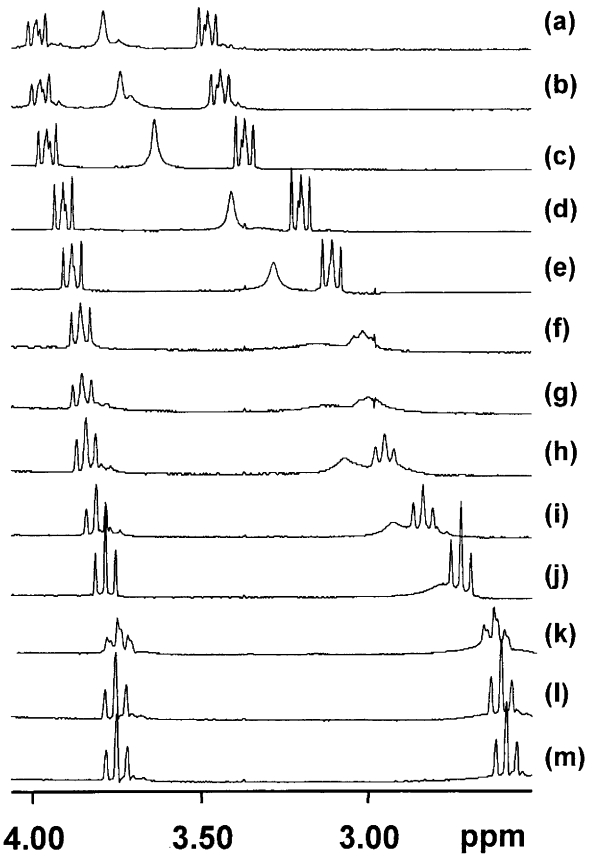

Fig. 5. ^1H NMR spectra at 200 MHz of *N,N'*-bis(2-hydroxyethyl)piperazine plotted versus pH at 24 °C and $I = 0.10$ mol dm^{-3} NaCl: (a) 2.48, (b) 2.97, (c) 3.47, (d) 4.06, (e) 4.45, (f) 5.28, (g) 6.12, (h) 7.01, (i) 7.54, (j) 7.96, (k) 8.44, (l) 8.97, (m) 11.04.

as well as into less intense triplets (**a'**) and (**b'**) (Fig. 1). The difference in the chemical shifts between the triplets (**a**) and (**a'**) as well as (**b**) and (**b'**) increases from 2.1 to 9.4 Hz in the course of the first protonation. The intensities of the signals are unequal, and the ratio of the

intensities varies. The coupling constants $^3J_{ab}$ and $^3J_{a'b'}$ have average values of 6.0 Hz.

During the second protonation (pH 5–2.4) the methylene proton resonances (**a**) and (**b**) as well as (**a'**) and (**b'**) appear as second-order AA'XX' multiplets. This was simulated using the program PERCH.[29] During the protonation the difference in the chemical shifts of these two unequal resonances (**a**) and (**a'**) as well as (**b**) and (**b'**) increases from 8.8 to 10.7 Hz. The intensity of the high-field resonance is about 20% from the low-field signal. The piperazine ring methylene resonance (**c**) has also split into two unequal singlets.

$^{13}C\{^1H\}$ NMR data are shown in Table 5. All the carbon resonances are sharp in the non-protonated form at pH 11.00, but the broadening is extensive at lower pH values (Fig. 6). Simultaneously, small satellites appear near to the two side-chain resonances. The appearance of the satellites is the clearest in the case of the resonance assigned to the methylene carbon bound to nitrogen.

These phenomena are typical for cyclic amines. The protonation of the amine nitrogen serves to slow down the dynamic equilibria so that the different conformations of the compounds are visible in the NMR spectrum; for example, the *N*-methylated piperidines show both the axial and equatorial protonated forms.[30] The small differences between the unequal proton triplets in our case are typical for the axial and equatorial conformations in the side chains of the six-membered rings.[31] Borane adducts show an analogous phenomenon in organic solvents. *N,N'*-dimethylpiperazine forms two different BH_3 adducts: 60% are in the equatorial–equatorial form and 40% in the equatorial–axial form.[32] Our NMR results also indicate the coexistence of the two major conformations regardless of the degree of protonation in the solution (Fig. 7). This was modeled using molecular mechanics calculations.[33] The total energy order of the different conformations of the protonated forms was equatorial–equatorial < equatorial–axial < axial–axial. Therefore, the major conformers in solution are equatorial–equatorial and equatorial–axial.

The two different protonation constants (Table 2) from (**a**) and (**a'**) resonances of *N,N'*-bis(2-hydroxyethyl)piperazine imply different proton affinities in different conformations. The protonation constants from the more intense resonance (**a**) are assigned to the equatorial–equatorial form and the constants from the less intense resonance (**a'**) are assigned to the equatorial–axial conformations (Fig. 7).

Table 5. $^{13}C\{^1H\}$ NMR of *N,N'*-bis(2-hydroxyethyl)piperazine in H_2O.

pH	δ_C (ppm) (O–CH_2)	δ_C (ppm) (N–CH_2)	δ_C (ppm) (ring–CH_2)
11.00	59.4	58.7	52.4
7.76	58.9	57.8	51.6
5.97	58.4	57.12, 56.99, 56.83	50.8
3.70	58.6	56.07, 55.78, 55.47	49.4
1.88	58.6	55.82, 55.47, 55.17	49.0

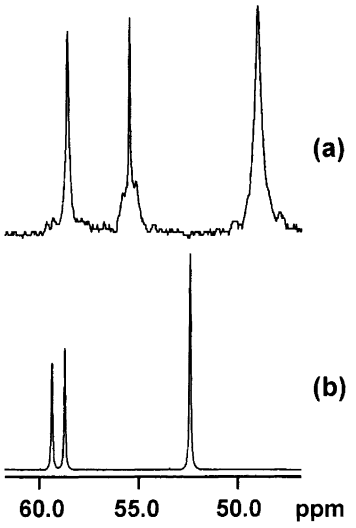

Fig. 6. $^{13}C\{^1H\}$ NMR spectra of *N,N'*-bis(2-hydroxyethyl)piperazine plotted versus pH in H_2O: (a) pH 1.88 and (b) pH 11.00.

Ring inversion. We have conducted a detailed study of the fluxionality[34] of *N,N'*-bis(2-hydroxyethyl)piperazine by recording the ^1H NMR spectra from −90 to 40 °C in a 1:1 (v:v) acetone–methanol solution. The temperature dependence is shown in Fig. 8. The singlet of the methylene protons of the piperazine ring at 2.4 ppm broadens and finally disappears to the base line when the temperature is decreased from 40 to 0 °C. Very broad resonances begin to grow at ca. 2.8 and 2.07 ppm at −20 °C. The other part of the resonance is partially obscured by the acetone resonance (ca. 2.05 ppm). These two resonances begin to sharpen and split at −30 °C, and both resonances are split into doublets at −50 °C. We observe the splitting of 8.0 Hz, which is reasonable for the geminal coupling constant between the axial and equatorial protons in six-membered rings. The chemical shift difference between the two signals is about 0.73 ppm. The chemical shift difference of 0.63 ppm was observed for *N,N'*-dimethylpiperazine in dichloromethane and the coalescence temperature was −8.5 °C.[35] The piperazine methylene proton resonances coalescence at about 0 °C and it is therefore possible to calculate the rate constant at this temperature. The two triplets of the 2-hydroxyethyl side chain methylenes sharpen during the cooling from 40 to −50 °C and the coupling constant ^3J has the average value of 6.0 Hz. Upon cooling to −90 °C the OH group resonance, that begins to grow at 5.3 ppm at −50 °C, is shifted downfield. At the same time the side-chain triplet from the methylene protons adjacent to the OH group is transformed into a quartet and the other triplet broadens.

The following parameters are obtained for *N,N'*-bis(2-hydroxyethyl)piperazine in 1:1 (v:v) acetone–methanol solution at 273 K: $k_{coal} = 652 \pm 10\ s^{-1}$, $\Delta G^{**} = 51.9 \pm 0.1\ kJ\ mol^{-1}$, $\Delta H^{**} = -2.5 \pm 0.1\ kJ\ mol^{-1}$ and

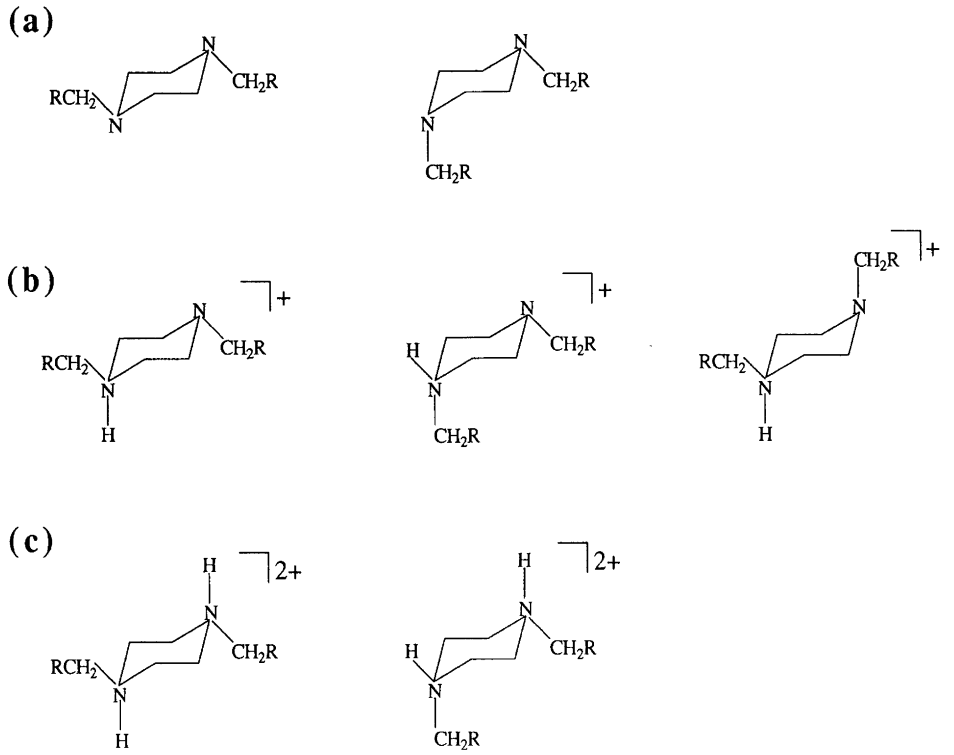

Fig. 7. Conformational changes in the *N,N'*-disubstituted piperazine, R = CH_2OH: (a) non-protonated, (b) mono-protonated and (c) di-protonated.

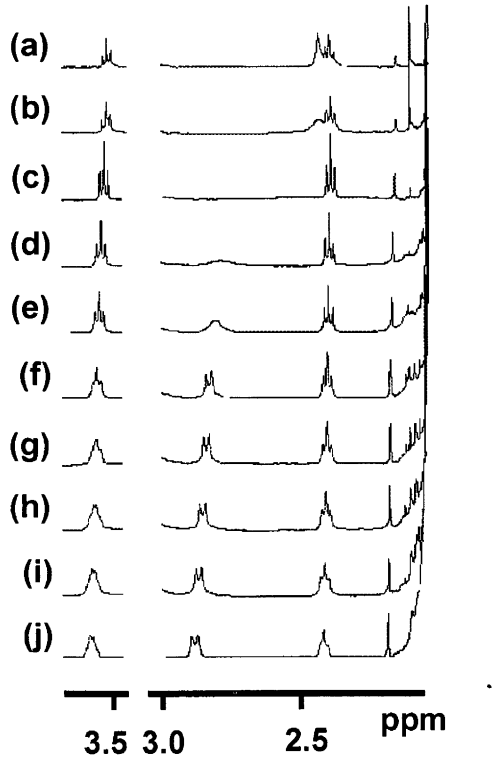

Fig. 8. ^1H NMR spectra at 400 MHz of *N,N'*-bis(2-hydroxyethyl)piperazine in the temperature range 40 to −90 °C in 1:1 (v:v) acetone–methanol solution: (a) 40, (b) 24, (c) 0, (d) −20, (e) −30, (f) −50, (g) −60, (h) −70, (i) −80 and (j) −90 °C.

$\Delta S^{**} = -199.7 \pm 0.2$ J K^{-1} mol^{-1}. It has previously been reported that $\Delta G^{**} = 52.7$ kJ mol^{-1} is obtained for *N,N'*-dimethylpiperazine in dichloromethane.[35] The substitution on heteroatoms seems to raise the ΔG^{**}-value, as exemplified by 42.3 kJ and 49.8 kJ mol^{-1} for piperidine and *N*-methylpiperidine, respectively.[36] This is consistent with our value of *N,N'*-bis(2-hydroxyethyl)piperazine. The solvent does not have a large effect on the ΔG^{**}-value. It probably plays a more significant role in determining whether the ring inversion is enthalpy- or entropy-driven. The great negative entropy of activation may indicate a greater degree of ordering in the transition state than in the initial state because of an increase in solvation through hydrogen bonding in the acetone–methanol mixture during the activation process. The coalescence temperature in the aqueous solution of *N,N'*-bis(2-hydroxyethyl)piperazine is ca. 297 K (Fig. 5), which is higher than in acetone–methanol mixture, because water has more effective hydrogen bonding than the acetone–methanol mixture during the activation process.

Acknowledgements. We are grateful to Dr. H. Rönkkömäki for a critical appraisal of the thermodynamic data. Financial aid from the Ministry of Education of Finland (to V.H.) is gratefully acknowledged.

References

1. Kaim, W. and Schwederski, B. *Bioinorganic Chemistry: Inorganic Elements in the Chemistry of Life*, 1st Edn., John Wiley and Sons, Chichester 1995.

2. Kushner, S. *J. Org. Chem. 13* (1948) 144.
3. Doadrio, A., Craciunescu, D., Ghirvu, C. and Nuno, J. C. *An. Quim. 73* (1977) 1220.
4. Vega, C. A. and Bates, R. G. *Anal. Chem. 48* (1976) 1293.
5. Chenevert, R. and Plante, R. *Synthesis* (1983) 847.
6. Larkins, H. L. and Hamilton, A. D. *Tetrahedron Lett.* (1986) 2721.
7. Krakowiak, K. E., Bradshaw, J. S., Jiang, W., Dalley, N. K., Wu, G. and Izatt, R. M. *J. Org. Chem. 56* (1991) 2675.
8. Kihara, N., Saigo, K., Kabata, Y., Ohno, M. and Hasegawa, M. *Chem. Lett.* (1989) 1289.
9. Bazzicalupi, C., Bencini, A., Fuzi, V., Micheloni, M. and Vantacoli, B. *J. Chem. Soc., Chem. Commun.* (1994) 1119.
10. Wade, P. W. and Hancock, R. D. *J. Chem. Soc., Dalton Trans.* (1990) 1323.
11. Hancock, R. D., Ngwenya, M. P., Evers, A., Wade, P. W., Boyens, J. C. A. and Dobson, S. M. *Inorg. Chem. 29* (1990) 264.
12. Wade, P. W., Hancock, R. D., Boyens, J. C. A. and Dobson, S. M. *J. Chem. Soc., Dalton Trans.* (1990) 483.
13. Hancock, R. D., Ngwenya, M. P., Wade, P. W., Boyens, J. C. A. and Dobson, S. M. *Inorg. Chim. Acta 164* (1989) 73.
14. Hancock, R. D., Dobson, S. M., Evers, A., Wade, P. W., Ngwenya, M. P., Boyens, J. C. A. and Wainwright, K. P. *J. Am. Chem. Soc. 110* (1988) 2788.
15. Jeffery, G. H., Bassett, G., Mendham, J. and Denney, R. C. *Vogel's Textbook of Quantitative Chemical Analysis*, 5th Edn., Longman, Avon 1989, pp. 186 and 311.
16. Ginstrup, O. *Chem. Instrum. 4* (1973) 141.
17. Sjöberg, S., Hägglund, Y., Nordin, A. and Ingri, N. *Marine Chem. 13* (1983) 35.
18. Ingri, N. and Sillen, L. G. *Ark. Chem. 23* (1964) 97.
19. Arnek, R., Sillen, L. G. and Wahlberg, O. *Ark. Chem. 31* (1969) 353.
20. Brauner, P., Sillen, L. G., and Whiteker, R. *Ark. Chem. 31* (1969) 365.
21. Eriksson, G. *Anal. Chim. Acta 112* (1979) 375.
22. Rossotti, H. S. *Talanta 21* (1974) 809.
23. Sigmaplot Scientific Graphing System Version 4.0, Jandel Corporation, 1986–1989.
24. Gunther, H. *NMR Spectroscopy*, 2nd Edn., Wiley, Chichester 1995, pp. 343.
25. Creyf, H. S. and van Poucke, L. C. *Thermochem. Acta 4* (1972) 485.
26. Aruga, R. *Inorg. Chem. 19* (1980) 2895.
27. Houngbossa, K. and Berthon, G. *Bull. Soc. Chim. Fr.* (1974) 2418.
28. Pouchet, J. C. *The Aldrich Library of NMR Spectra*, 2nd Edn., Aldrich Chemical Co. Inc., Milwaukee 1983, p. 328.
29. Laatikainen, R., Niemitz, M., Weber, U., Sundelin, J., Hassinen, T. and Vepsäläinen, J. *J. Magn. Reson., Ser. A 120* (1996) 1.
30. Eliel, E. L., Kandasamy, D., Chen-yu Yen and Hargrave, K. D. *J. Am. Chem. Soc. 102* (1980) 3698.
31. Jones, R. A. Y., Katritzky, A. R., Ostercamp, D. L., Record, K. A. and Richards, A. C. *J. Chem. Soc., Perkin Trans. 2* (1972) 34.
32. Flores-Parra, C. A., Farfan, N., Hernandez-Bautista, I., Fernandez-Sanchez, L. and Contreras, R. *Tetrahedron 34* (1991) 6903.
33. Spartan Version 4.0. Wavefunction, Inc., 1995.
34. Dijkstra, G. D. H. *Recl. Trav. Chim. Pay-Bas 112* (1993) 151.
35. Harris, K. R. and Spragg, R. A. *J. Chem. Soc. Chem. Commun.* (1966) 314.
36. Eliel, E. L. and Wilen, S. H. *Stereochemistry of Organic Compounds*, 1st Edn., John Wiley and Sons, New York 1994, pp. 668 and 741.

Received May 11, 1998.